

Monitoring Land Cover Changes in Halabja City, Iraq

Jwan Al-doski, Shattri B. Mansor and Helmi Zulhaidi Mohd Shafri
*Geo-spatial Information Science Research Center (GIS RC), Faculty of Engineering
Universiti Putra Malaysia, 43400 UPM, Serdang, Selangor, Malaysia*
Jwan-83@hotmail.com, shattri@gmail.com, helmi@eng.upm.edu.my

Abstract-This paper presents land use / land cover changes of the Halabja city in the north part of Iraq over 1986 to 1990 by utilizing multi-temporal remote sensing imagery. Halabja city has been facing severe land use/land cover changes following a series of wars beginning with Iraq-Iran war (1980-1988) to the just concluded invasion of Iraq (March 19, 2003 – 2011). In this study, multi-temporal Landsat images (TM) between the years of 1986 and 1990 were used. All images are rectified and registered to Universal Transverse Mercator (UTM), zone 38N and WGS_84 datum. Hybrid classification as a combine of k-Means and Maximum Likelihood Classification (MLC) algorithms were applied to classify the images in five different land cover categories: water body, cultivated area, shrub land, urban area and bare land. Quantitative analysis was conducted by using post-classification change detection technique. The results show an overall accuracy for 1986 and 1990 images are 92.2% and 96.8% respectively. During 1986 to 1990 land use / land cover changes a lot with a huge decrease about 40.8% in cultivated area whereas, urban area, Shrub Land and bare land classes increased by 57.9 %, 67.1 % and 14 % respectively.

Keywords — Landsat TM, Land Use/ Land Cover, K-Means, Hybrid Classification, Maximum Likelihood Classification.

I. INTRODUCTION

Land use/ land cover (LULC) is a fundamental environmental variable for understanding the causes and trends of human and natural processes [1]. Basically LULC consists of two terms; Land use (LU) and land cover (LC). Land cover is that which covers the surface of the earth such as water, snow, forest, grassland, and bare soil; while land use describes how the land cover is modified into use for example agricultural land, built up land etc. [2]. There are many approaches to monitor LULC ; traditional techniques such as field survey and remotely sensed images such as satellite images, aerial photographs and others.

Satellite remote sensing is the most common data source for detecting, quantifying, and mapping LULC changes at various scales [4] because its availability and repetitive data acquisition, improved quality of multi-spatial and multi-temporal remote sensing data at different spatial,

spectral, and digital format suitable for computer processing and new analytical techniques [5]. Hence, detecting temporal changes of LULC by observing them at different times, is one of the most important applications of earth-orbiting Satellite sensors.

Recently, there are numerous satellites in operation among them medium resolution satellite imagery such as Landsat that has been used broadly by many researchers for LULC changes because it provides a historical and continuous record of imagery the uniqueness of the dataset as the only long-term digital archive with a medium spatial resolution and relatively consistent spectral and radiometric resolution [17]. The successful use of satellite remote sensing for LULC change detection depends upon an adequate understanding of landscape features, imaging systems, and methodology employed in relation to the aim of analysis. A number of studies have attempted to use Landsat data to address LULC change for example Gilman and Baz used Landsat TM and Landsat Geo-Cover LC satellite images used for detecting land-cover changes in the Istanbul metropolitan area [18]. While, Wen used Landsat Multi-Spectral System (MSS) to derive land cover information and changes in Guam, USA [19].

Change detection using remote sensing data is the process of identifying and examining temporal, spatial and spectral changes in the pixels [6]. Continual, historical, and precise information about the LULC changes of the Earth's surface is extremely important for government agencies and research institutions and organizations that have to deal with land management decisions as well as to develop strategies for sustainable development and improve the livelihood of cities [3]. Change detection had become a key in many applications

related to LULC changes for instance, agricultural monitoring [7], deforestation assessment [8], yield estimation and assessment [9], coastal zone changes [10], land degradation detection [11], vegetation mapping [12], wetland landscape changes [13], snow cover changes [14], urban change detection [15], burned area [16] and other applications.

Various changes detection techniques have been developed and used for monitoring changes in LULC from remotely sensed data [5,20,21] such as Image Differencing (ID) [22], RGB-NDVI Change Detection Method [23,24] , Band Image Differencing [25], Principal Component Differencing (PCD) [26], Change Vector Analysis (CVA) [27], Vegetation Index Differencing (VID) [28] and others. Generally, change detection techniques can be grouped into two: based on the classification of the input data and based on the radiometric value change between acquisition dates [3]. Recently, LULC information is obtainable by using classification techniques [5]. Image classification is a process of assigning pixels to classes [4]. According to whether prior knowledge is needed before classification, classification methods are usually grouped into two categories; the unsupervised classification and the supervised classification. One of the common change detection classification bases is post-classification technique [5]. The post-classification (map-to-map comparison) method identifies conversion from one LULC type to another with little information on the intensity of such changes.

The post - classification method was employed typically, based on traditional unsupervised and supervised classification algorithms in different areas around the world. More recently, it was utilized based on newest classification algorithms for different purposes as to quantify land cover change, improve spectral classification, reduce the classification error propagation and improve the land-use and land-cover change classification accuracy such as using automated classification approach [29], Rx Classification Algorithm [30], Object-Based Classification[31] , Standardized Object Oriented Automatic Classification (SOOAC) Method Based on Fuzzy Logic [32], Knowledge-

Based Stratified Classification[33], Artificial Neural Networks[34], Decision Tree Classification(DT) Method [35], and Hybrid classifier [36].

In this study, post-classification change detection technique utilized based on hybrid classification as integration of k-means and Maximum Likelihood Classifier (MLC) to detect LULC changes in Halabja city, Iraq.

The rest of the paper is organized into four sections; next section gives a general description about the study area. In section III explaining Landsat data sets used with a short explanation about classification algorithms and post-classification change detection techniques. A methodology is presented in section IV. Section V focuses on data analysis and result presentation forms. Finally, a brief conclusion of this research is written in section VI.

II. DESCRIPTION OF STUDY AREA

Halabja city, with an area about 1258.74 km² and a population about 70,000 people, is located in northeast of Iraq, about 80 kilometers from southeastern of Sulaimanya city, 241km northeast of the capital city Baghdad and about 16 Km away from the Iraq - Iran border. Geographically, Halabja lies within 35°04'22.5" and 35°20'29.7" latitudes and 45°37'39.4" and 46°07'10.2"E longitudes (Fig.1). Topographically, it lies in southeastern Sharazur plain, surround by Hawraman and Balambo mountains to the north and south respectively. To the west, it is bordered by the man-made lake (Sirwan), which is fed by Sirwan, Zalm, and Tanjro rivers, emptying via Darbandikhan dam into the Diyala river, and finally into the mighty Tigris as it flows toward the Arabic Gulf. These rivers are mainly fed by local rainfalls. The climate in Halabja is typified by hot weather in the summer with temperature ranging from 15⁰ C to 35⁰ C and sometimes up to 40⁰ C and bitterly cold during winter while it has a moderate climate in other season.

Toward the end of Iraq-Iran war, exactly on March 16, 1988, Halabja city and surrounding villages such as Khormal were attacked with

chemical weapons and artillery fire. The attack is said to have included the Nerve Agents, Tabun, Sarin, and VX, as well as Mustard Gas [39, 40]. After the attack, the Iraqi army moved in and completely destroyed the city [41]. At least 5,000 people died as an immediate result of chemical attack and it is estimated that 7,000 people were injured or suffered long term illness [42]. Most of the victims of the attack on the Halabja city were Kurdish civilians [43]. Until this moment, Halabja attack still remains the largest chemical weapons attack directed against a civilian-populated area in history [44]

Precipitation varies between 700 and 3,000 mm a year on the high plateau between the mountain chains. Despite this, much of the region is fertile area covered with forest vegetation with the historical antecedent of exported grain and livestock. Moreover, mountainous region with cold climate gets annual precipitation that is suitable to keep up temperate forests and shrubs [37, 38].

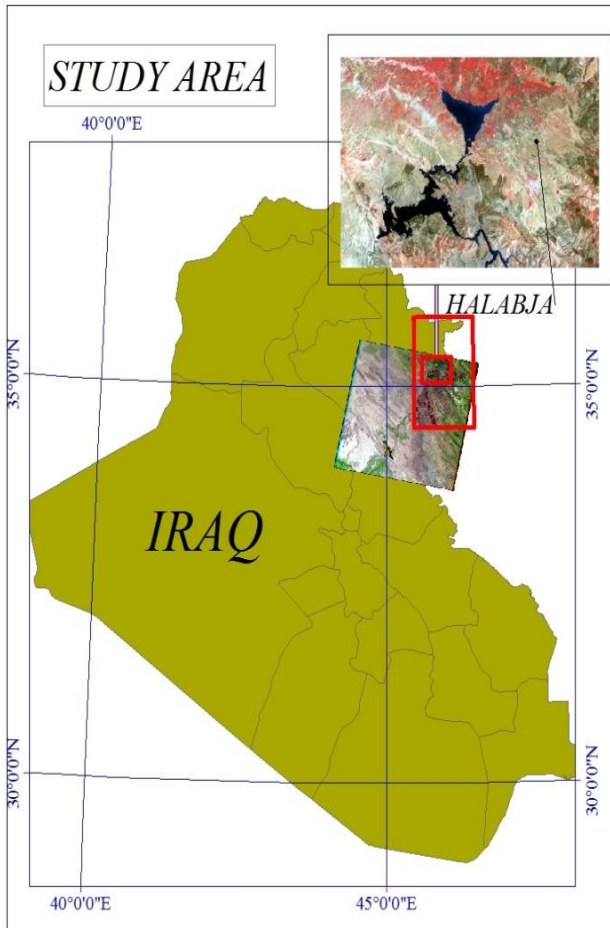


FIGURE 1. MAP OF THE STUDY AREA

This Figure Shows the Landsat Satellite Full Scene over Sulaimanya and Interested Area (Halabja City)

III. MATERIAL AND METHODS

A. Data Used

Landsat satellites have been collecting images of the earth's surface for more than forty years. NASA (National Aeronautics and Space Administration) launched the first Landsat satellite in 1972, and the most recent one, Landsat 7, in 1999. Currently, only the Landsat 5 and 7 are still operating normally. Landsat 5 carries the Thematic Mapper (TM) sensor with 30m visible and IR (Infra-Red) bands and one thermal-IR band, with a 120m spatial resolution.

The data used in this study include two Landsat Thematic Mapper (TM) images acquired on June 14, 1986 and June 9, 1990 for path 168, row 36 see (table 1). These images are freely available from the Landsat archive in the United States Geological Survey (USGS) website (<http://glovis.usgs.gov>). In order to reduce the impact of sun angle differences and vegetation phenology differences, images were acquired with the same sensor and approximately the same time of the year during the fall growing season [45, 46]. Reference data consists of high resolution historical images were downloaded from Google earth and used mainly during the image classification process and accuracy assessment.

TABLE 1

LANDSAT SCENES USED FOR THE ANALYSIS

Images	Satellite Instrument	Date	Pixel Size (m)
1986 image	Landsat 5 TM	June 14, 1986	30x30
1990 image	Landsat 5 TM	June 09, 1990	30x30
Base Image 2000 image	Landsat 7 ETM+	June 28, 2000	30x30

B. Methods

1. K-means

This algorithm, classes are determined statistically by assigning pixels to the nearest cluster mean based on all available bands. It is relatively straightforward and has considerable

intuitive appeal. However, the output of this technique could be influenced by the number of cluster centres specified, the choice of the initial cluster centre, the sampling nature, the geometrical properties of the data and clustering parameters [47].

In K-Means, a sequence of iteration starts with an initial set $C^{(0)}$ [48], In each iteration t all $c \in C$ pixels are assigned to one of the clusters $S_k^{(t)}$ as defined by nearest neighbour principle. A new centre $C_k^{(t)}$ for a cluster is computed as follows (Eq. 1):

$$c_j^{(t+1)} = \frac{1}{N_j} \sum (c_i | c_i \in S_j^{(t)}) \quad \text{Eq 1}$$

2. Maximum-Likelihood Classifier (MLC)

The maximum likelihood classifier (MLC) is a pixel-based method and it is considered as one of the most popular classification methods in remote sensing, in which a pixel with the maximum likelihood is classified into the corresponding class. The MLC procedure was chosen as a classification method in this study because of its ready availability and the fact that it did not require an extended training process [49]. The MLC is based on the assumption that the members of each class are normally distributed in feature space. In the case of normal distributions, the likelihood can be expressed in (Eq.2) as follows:

$$Lci(x) = \frac{1}{(2\pi)^{k/2} |V_i|^{1/2}} \exp \left[-\frac{1}{2} (x - \bar{x}_i)^t V_i^{-1} (x - \bar{x}_i) \right] \quad \text{Eq2}$$

Where $Lci(x)$ = likelihood of x belonging to class i ; k = number of image characteristic; x = image data of k ; \bar{x}_i = mean vector of class i ; V_i = variance- covariance matrix of class i .

3. Post-classification comparison technique

The most obvious method of change detection is post-classification comparison which determines the difference between independent classified images for each of the dates in question [6]. It enables the recognition, quantifying and mapping

of the type of land cover change as well as the kind of land cover changes that have occurred. However, the accuracy of this change detection technique is only as good as the result of the multiplication of the accuracies of each individual classification [5].

IV. METHODOLOGY

The methodology in this study involves four steps; pre- processing, image classification and creation land cover maps for 1986, and 1990, accuracy assessment and implementation of change detection technique.

A. Pre-processing

Pre-processing of satellite images has the unique goal of establishing a more direct linkage between the data and biophysical phenomena [3]. The pre-processing adopted to take geometric correction into consideration, image registration, radiometric correction, and atmospheric correction [50].

All Landsat data used in this study were acquired under clear atmospheric conditions (Figure 2). The images were Geo-coded to the Universal Transverse Mercator (UTM) coordinate system, zone 38 and WSG84 Datum. Geometric correction was done using image-to-image method with a second-order polynomial by taking corrected Landsat 2000 images as a base image for all other images. A minimum of 24 regularly distributed ground control points (GCPs) was selected from the images. The transformation had a root mean square (RMS) error of 0.43 and 0.39 for 1986 and 1990 images respectively, indicating that the image was accurate to within one pixel. Resampling was performed using a nearest neighbour algorithm; this algorithm takes the value of the pixel in the input image that is closest to compute the coordinate. This method is fast and does not alter the original pixel values.

In the next step, the images were radiometrically normalized. For many change detection applications, radiometric correction is unnecessary, but variations in solar illumination conditions, in atmospheric scattering and absorption, and in detector performance need to be normalized [51]. In the course of this study, two images were

acquired by TM sensor and purchased from U.S. Geological Survey Imaging, which has processed the image data to a much higher degree of radiometric quality application. Further radiometric normalization will increase enhance radiometric resolution therefore, the relative radiometric correction method was applied to the three scenes.

Relativistic radiometric correction is a two –step processes: First: converting 8-bit satellite-quantized digital numbers (DN) to spectral radiance ($L\lambda$) by using equation 3.

$$L\lambda = LMIN + \frac{LMAX - LMIN}{QCALMAX - QCALMIN} \times QCAL - QCALMIN \quad \text{Eq3}$$

Where:

QCAL= the calibrated and quantized scaled radiance in

Units of (DNs)

LMIN = the spectral radiance at QCAL = 0

LMAX λ = the spectral radiance at QCAL = QCALMAX

QCALMIN= the minimum quantized calibrated pixel value

QCALMAX = the maximum quantized.

The resulting radiance ($L\lambda$) is in units of watts per square meter per steradian per micrometer ($W/(m^2 \cdot sr \cdot \mu m)$). Second: spectral radiance ($L\lambda$) values converted to top of atmosphere (TOA) reflectance units (P) using equation 2.

$$P = \frac{L\lambda \times d^2}{ESUN \times \cos s} \quad \text{Eq4}$$

Where:

$L\lambda$ = the spectral radiance

d = the Earth-Sun distance in astronomical units

ESUN λ = the mean solar Exo-atmospheric radiance

COSS = the solar zenith angle in degrees

LMIN λ , ESUN λ and LMAX λ were derived from values published [52, 53] .

Images acquired at different times usually have different amounts of haze and dust in the atmosphere. To overcome this problem dark object subtraction model of atmospheric correction techniques was applied.

B. Area Extraction and Image Enhancement

For extracting area of interest, all images were subset spatially to 1400 samples and 999 lines followed by image enhancement. Image enhancement is the modification of an image in order to alter its impact on the viewer [54]. The general aim of image enhancement is to highlight features of thematic interest such as water, vegetations, rock and soil properties, etc., as well as image enhancement makes the images more interpretable for specific applications. Generally, image enhancement changes the original digital value and it should be carried out after Geo-referencing. Major tools applied for the enhancement of the Landsat TM satellite data were histogram analysis and contrast stretching, edge enhancement, RGB-Coding and Principal Component Transformation.

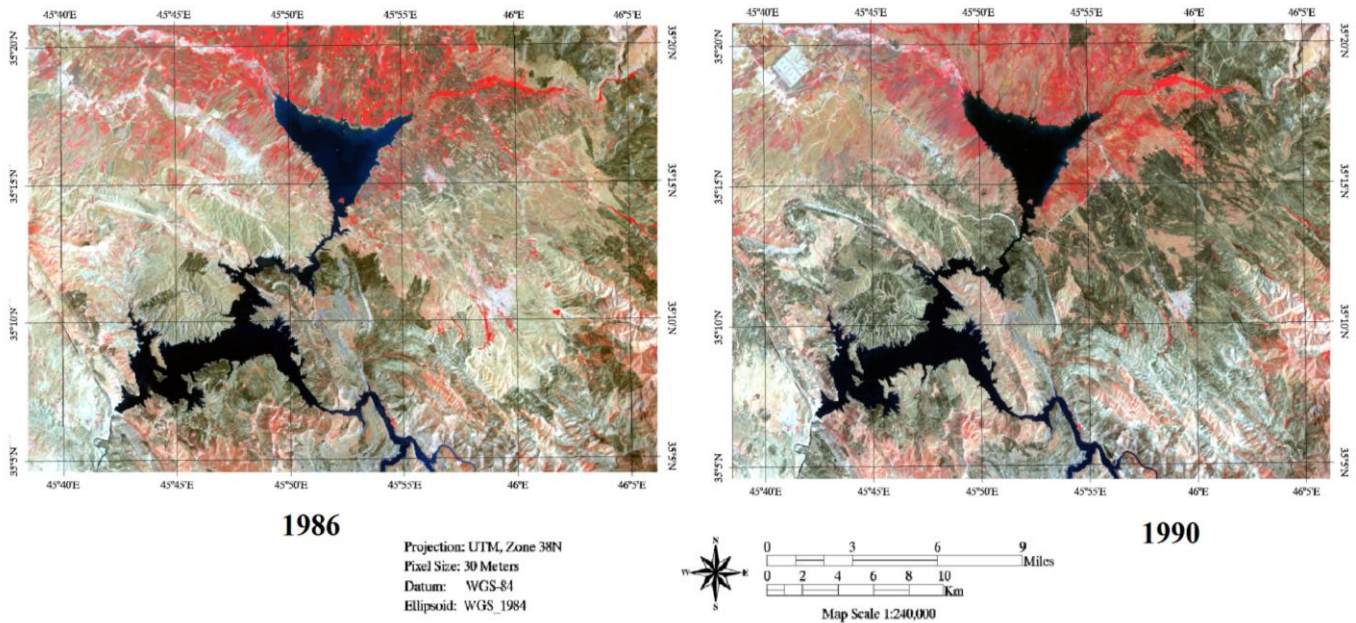


FIGURE 2. FALSE COLOR LANDSAT 5 TM IMAGES FOR 1986 AND 1990

C. Image Classification

Digital analysis and image classification are carried out using ENVI 4.8 and ArcGIS 9.3 softwares to produce thematic maps and analyze changes. Since 1970s, various classification approaches had been developed and employed to extract land cover information and monitor changes [55]. For this study, The Level-1 classification of Anderson scheme classification is adopted to prepare LULC maps, five land cover classes were intended to be mapped: Water Body, Shrub Land, Cultivated Area, Urban Area and Bare Land.

All data sets were classified by using k-means and maximum likelihood classification separately, the results of both techniques showed a poor accuracy as illustrated in table 2 so the classification by means of a hybrid classifier that combines both of the k-means and maximum likelihood classification techniques was performed in this paper.

The classification process involved three steps: the first stage of a hybrid classification is clustering, k-means algorithm as unsupervised classification that was adopted to generate forty different clusters from the Landsat data. This is an iterative approach of classification that was run for ten iterations on

the remaining unknown clusters from each step until all were classified.

Secondly, Cluster labelling was used to separate clusters into 5 land cover or an unknown class if the clusters could not be identified by plotting in spectral space and a visual check was made based on terrain knowledge; referring to Google earth.

Finally, once the 5 land cover classes were deemed satisfactory then they were entered as spectral signature into the supervised classification process. The maximum likelihood method as a supervised classification method run and the outputs were two thematic maps for 1986 and 1990 (the classified image).

D. Classification Improvement

Visual interpretation was adopted to improve classification accuracy and reduce misclassifications. This method has been proven in many researches for increasing classification accuracy and consequently the quality of the LULC maps produced [56]. In this study, we integrated a process involved applying an overlay operation using ENVI 4.8 of the initial LULC maps resulting from hybrid classification with the high resolution images from Google earth. Finally, we produced accurate LULC maps (Fig. 3).

E. Accuracy Assessments

Accuracy assessment involves statistical estimates obtained from remote sensing classification output and an independent reference dataset in order to measure the probability of error for the classified map. The popular method is named 'confusion matrix' method. Error matrix is included n by n , the rows of the matrix represent the classification points, the lines represent the reference points and the points in the main diagonal of the matrix are the correct points after classification [57].

A stratified random sampling design was adopted for the accurate assessment of both maps. The sample points were generated and their locations were chosen to represent different land cover classes in the area. In all, a total of 500 pixels was selected. In order to increase the accuracy of land cover mapping of the two images, all the pixels were checked and visually interpreted based on RGB color composition imagery and high spatial resolution images of Google earth. Generally, four measures of accuracy were tested in this study, namely the overall accuracy, user's accuracy, producer's accuracy and kappa index (K) used to estimate the results.

F. Change Detection

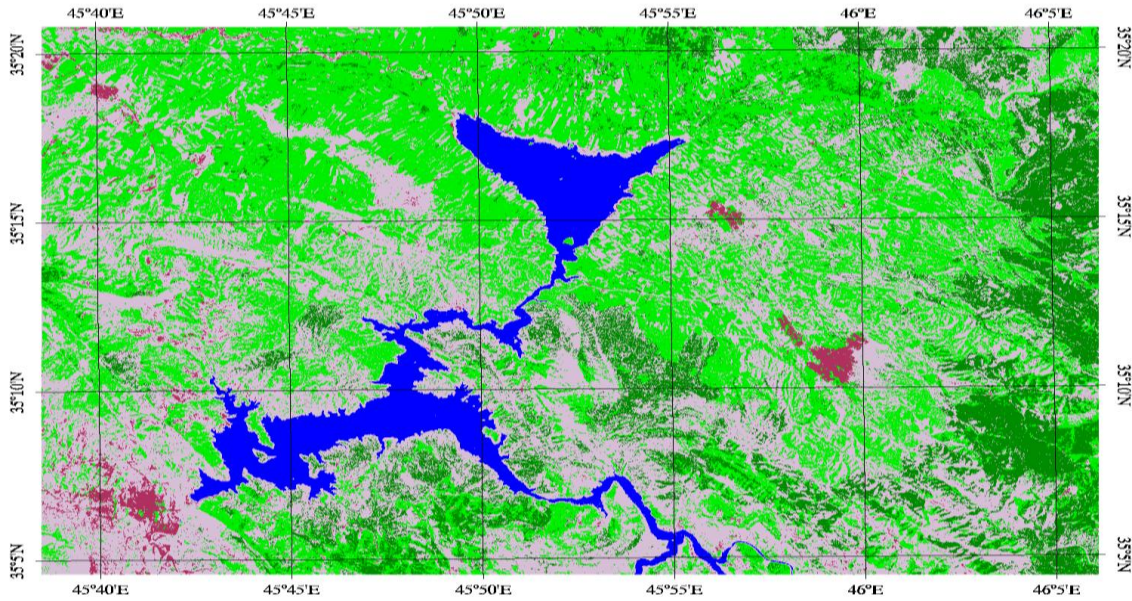
Change detection statistics used to compile a detailed tabulation of changes between two classification images. To perform change detection over a 4 year time period, the post-classification comparison change detection technique was employed. This technique is widely used and requires final classification maps with the highest accuracy possible to be compared pixel-by-pixel. One of the great advantages of the post classification technique is easy to use so that it allows the analyst to identify and understand the nature of the changes occurring in the study region [57]. In this study, Landsat TM data of both dates were independently classified using the hybrid classifier and the results compared using this technique to detect the differences between LULC maps 1986 and 1990 by taking 1990 as final map and 1986 initial map.

In comparison of the results of both techniques k-means and MLC as they were applied separately and tabulated in table 2 with the hybrid classification results. One can see clearly, the accuracy is increased by utilizing hybrid classification to generate LULC maps of the study area .

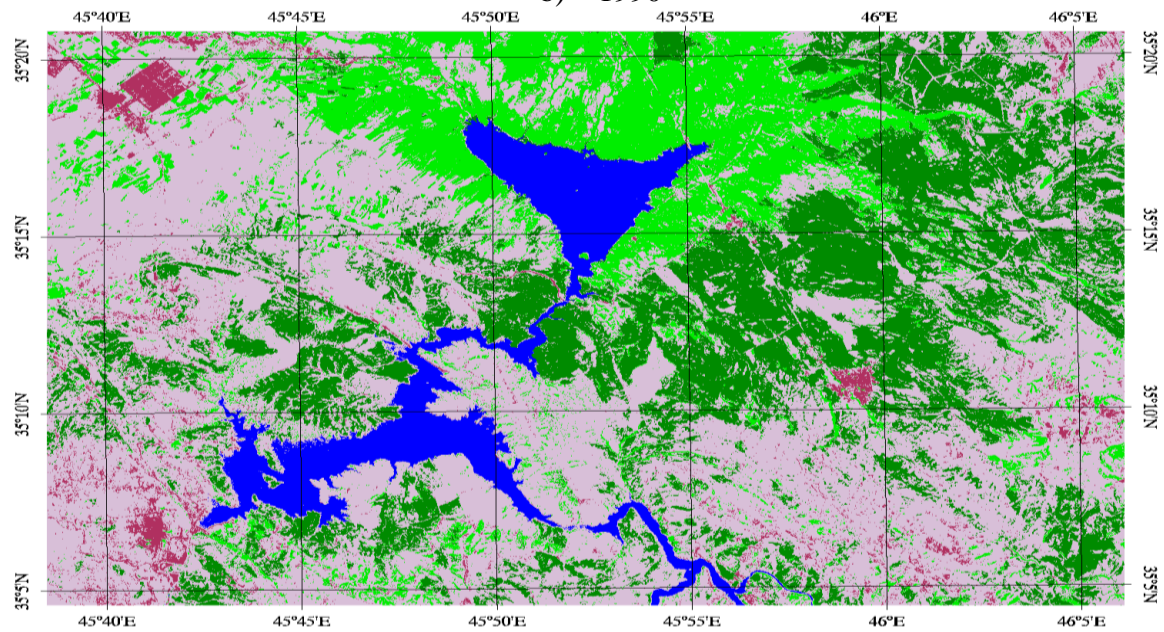
The error matrix of the LULC maps obtained for the years 1986 and 1990 by utilizing hybrid classification tabulated in tables 3 and 4 and Figures 4a and 4b show the map after the classification of different LULC changes over the Halabja city with the highest accuracy achieved. Tables 3 and 4 show for 1986 map, 461 by 500 pixels were correctly assigned with an overall accuracy that is about 92.2% and a kappa index of agreement of about 0.9. In comparison, 1990 map, 484 by 500 pixels were correctly assigned with an overall accuracy about 96.8% and a kappa index of agreement of about 0.96. In terms of both the producer and user's accuracies, the producer's accuracy (1986) exceeded 90% for all classes except the bare land about 79%, while the (1990) map exceeded 89% for all the classes. In the same vein, user's accuracies for both years and, for all the classes exceeded 83%. This implies that the hybrid classification gives the highest accuracy and the classes classified .

Table 5 shows the statistical analysis of LULC changes in the Halabja city from 1986 to 1990. From this table, it is obvious that there was a drastic change in planted/cultivated, shrub land, and urban area. Cultivated area decreases by 40.8% over the period. The total negative change of this class changed to the other class. Much of this change is in the shrub land, bare land and urban area. Inversely, urban area increases by 67.13% within the same period of time. This could be as a result of new settling development in new Halabja (Halabja taza) for the survivors who returned after the war. Consequently, a decrease in cultivated area is obvious, turning previously cultivated area to grow seasonal weeds and some eventually turn to barren land.

a) 1986



b) 1990



Projection: UTM, Zone 38N
 Pixel Size: 30 Meters
 Datum: WGS-84
 Ellipsoid: WGS_1984



Unclassified
 Water Body
 Planted/Cultivated Area
 Shrub Land
 Urban Area
 Bare land

FIGURE3. THE CLASSIFICATION MAPS FOR DIFFERENT LULC CLASSES OVER HALABJA IN (A) 1986 AND (B) 1990 USING HYBRID CLASSIFICATION (K-MEANS AND MAXIMUM LIKELIHOOD CLASSIFIERS)

TABLE2
 OVERALL ACCURACY AND KAPP FOR CLASSIFICATION ALGORITHMS

Classification Algorithms	Landsat 5TM 1986 Image		Landsat 5 TM 1990 Image	
	Overall Accuracy%	Kappa Coefficient%	Overall Accuracy%	Kappa Coefficient%
K-means Classification	68.8	0.61	86.6	0.8325
MLC Classification	62.8	0.535	68.2	0.6
Hybrid Classification	92.2	0.902	96.8	0.96

TABLE3
 ERROR MATRICES OF THE 1986 LULC MAP USING HYBRID CLASSIFICATION

LULC classes	Ground Truth (Pixels)						User Accuracy (%)
	Water	Planted/ Cultivated Area	Shrub Land	Urban Area	Bare Land	Total rows	
Water	100	0	0	0	0	100	100
Planted/Cultivated Area	0	90	8	0	1	99	90.91
Shrub Land	0	10	92	0	0	102	90.20
Urban Area	0	0	0	100	20	120	83.33
Bare Land	0	0	0	0	79	79	100
Total columns	100	100	100	100	100	461	
Produce Accuracy (%)	100	90	92	100	79		

TABLE4
 ERROR MATRIX OF THE 1990 LULC MAP USING HYBRID CLASSIFICATION

LULC classes	Ground Truth (Pixels)						User Accuracy (%)
	Water	Planted/ Cultivated Area	Shrub Land	Urban Area	Bare Land	Total rows	
Water	100	0	0	0	0	100	100
Planted/Cultivated Area	0	99	0	0	0	99	100
Shrub Land	0	0	96	0	0	96	100
Urban Area	0	0	2	89	0	91	97.80
Bare Land	0	1	2	11	100	114	87.72
Total columns	100	100	100	100	100	484	
Produce Accuracy (%)	100	99	96	89	100		

TABLE5.
 LAND COVER/ LAND USE AREA CHANGE WITHIN THE HALABJA CITY FROM 1986 TO 1990 (UNIT: SQUARE KM)

Land Cover Category	1986 Area	1990 Area	Area Change	Area Change %
Water	72.67	76.34	3.67	5.057
Planted/Cultivated Area	470.65	278.63	-192.02	-40.799
Shrub Land	171.89	271.53	99.64	57.968

Urban Area	22.75	38.03	15.28	67.135
Bare Land	520.78	594.20	73.42	14.099

VI. CONCLUSION

Through this study, the results indicate that multi-temporal Landsat time series has great potential for analysis LULC changes in Halabja city, north part of Iraq. In addition, hybrid classification as a combination of k-means and maximum likelihood algorithms was presented and tested. The results show the efficiency of hybrid classification to produce high accuracy LULC maps over the Halabja city for the 1986 and 1990. Furthermore, the post-classification change detection method proposed here proved to be very efficient to identify land cover changes during the period of 1986-1990. Planted/Cultivated class decreased by 40.8%. Whereas, the urban area, Shrub Land and bare land classes increased by 57.9 %, 67.1 % and 14 % respectively.

ACKNOWLEDGMENT

Appreciation goes to Prof, Dr. Shattri.B.Mansor for his encouragement and support. Thanks are also extended to Dr. Helmi Zululhaidi. Bin Mohd Shafri. Extended thanks go to University Putra Malaysia technical staffs for their supports.

REFERENCES

- [1] W. B. Meyer and B. L. Turner, "Human population growth and global land-use/cover change," *Annual Review Ecology and Systematics*, vol. 23, 1992, pp. 39-61.
- [2] Cihlar, J. 2001 R. E. Kennedy, P. A. Townsend, J. E. Gross, W. Cohen, P. Bolsrad, and T. Wang, et al., "Remote sensing change detection tools for natural resource managers: Understanding concepts and tradeoffs in the design of landscape monitoring projects," *Remote Sensing of Environment*, vol. 113 (7), 2009, pp. 1382-1396.
- [3] P. Coppin, I. Jonckheere, K. Nackaerts, and B. Muys, "Digital change detection methods in ecosystem monitoring: a review," *International Journal Remote Sensing*, vol. 25 (9), 2004, pp. 1565-1596.
- [4] J. F. Mas, "Monitoring land-cover changes: a comparison of change detection techniques," *Int. J. Remote Sens.*, Vol. 20, pp. 139-152, 1999.
- [5] D. Lu, P. Mausel, E. Brondizio and E. Moran, "Change detection techniques," *Int. J. Remote Sens.*, Vol. 25, pp. 2365-2407, 2004.
- [6] A. Singh, "Digital change detection techniques using remotely-sensed data," *Int. J. Remote Sens.*, Vol. 10, pp. 989-1003, 1989.
- [7] G. R. Gibson, "Three Decades of Agricultural Land Use and Land Cover Change in Iraq," *War and Agriculture: Three Decades of Agricultural Land use and Land Cover Change in Iraq*, 2012.
- [8] T. N. K. D. Binh, N. Vromant, N. T. Hung, L. Hens and E. Boon, "Land cover changes between 1968 and 2003 in Cai Nuoc, Ca Mau peninsula, Vietnam," *Environ. Dev. Sustainability*, vol. 7, pp. 519-536, 2005.
- [9] P. V. K. Rao, V. V. Rao and L. Venkataratnam, "Remote sensing: A technology for assessment of sugarcane crop acreage and yield," *Sugar Tech*, vol. 4, pp. 97-101, 2002.
- [10] Hongquan Xie, Yanyan Zhang and Xia Lu, "Land use/cover change study of lianyungang coastal zone based on remote sensing," in *Geoinformatics, 2011 19th International Conference on*, 2011, pp. 1-5.
- [11] S. Chen and P. Rao, "Land degradation monitoring using multi temporal Landsat TM/ETM data in a transition zone between grassland and cropland of northeast China," *Int. J. Remote Sens.*, vol. 29, pp. 2055-2073, 2008.
- [12] J. Müllerová, "Use of digital aerial photography for sub-alpine vegetation mapping: A case study from the Krkonoše Mts., Czech Republic," *Plant Ecol.*, vol. 175, pp. 259-272, 2005.
- [13] Wang Huiliang, Wang Xuelei, Xiao Rui and Mo Minghao, "A study on the change of wetland landscape pattern in honghu city by using 3S method," in *Environmental Science and Information Application Technology, 2009. ESAT 2009. International Conference on*, 2009, pp. 167-170.
- [14] G. Singh and G. Venkataraman, "LOS PALSAR data analysis of snow cover area in himalayan region using four component scattering decomposition technique," in *Recent Advances in Microwave Theory and Applications, 2008. MICROWAVE 2008. International Conference on*, 2008, pp. 772-774.
- [15] G. Camps-Valls, L. Gómez-Chova, J. Muñoz-Marí, J. L. Rojo-Álvarez and M. Martínez-Ramón, "Kernel-based framework for multitemporal and multisource remote sensing data classification and change detection," *Geoscience and Remote Sensing, IEEE Transactions on*, vol. 46, pp. 1822-1835, 2008.
- [16] J. I. Z. Gitas, G. H. Mitri and G. Ventura, "Object-based image classification for burned area mapping of Creus Cape, Spain, using NOAA-AVHRR imagery," *Remote Sens. Environ.*, vol. 92, pp. 409-413, 2004.
- [17] P. Chen, X. Lu, S. Liew and L. Kwok, "Quantification of land cover change and its impact on hydro-geomorphic processes in the upper yangtze using multi-temporal landsat imagery: An example of the minjiang area," in *Geoscience and Remote Sensing Symposium, 2002. IGARSS'02. 2002 IEEE International*, 2002, pp. 1216-1218.
- [18] A. Geymen and I. Baz, "Monitoring urban growth and detecting land-cover changes on the Istanbul metropolitan area," *Environ. Monit. Assess.*, vol. 136, pp. 449-459, 2008.
- [19] Y. Wen, "Data application of multi-temporal and multi-source data for land cover change detection in guam, USA," in *Geoinformatics, 2011 19th International Conference on*, 2011, pp. 1-4.
- [20] J. F. Mas, "Monitoring land-cover changes: a comparison of change detection techniques," *Int. J. Remote Sens.*, vol. 20, pp. 139-152, 1999.
- [21] D. Lu, E. Moran, S. Hetrick and G. Li, "Land-Use and Land-Cover Change Detection," *Advances in Environmental Remote Sensing: Sensors, Algorithms, and Applications*, vol. 7, pp. 273, 2010.
- [22] M. Rymasheuskaya, "Comparison of several change detection methods for monitoring land cover dynamics in belarus," in *Analysis of Multi-Temporal Remote Sensing Images, 2007. MultiTemp 2007. International Workshop on the*, 2007, pp. 1-3.
- [23] S. A. Sader and J. C. Winne, "RGB-NDVI colour composites for visualizing forest change dynamics," *Int. J. Remote Sens.*, vol. 13, pp. 3055-3067, 1992.
- [24] D. Lu, P. Mausel, M. Batistella and E. Moran, "Land cover binary change detection methods for use in the moist tropical region of the Amazon: a comparative study," *Int. J. Remote Sens.*, vol. 26, pp. 101-114, 2005.
- [25] D. Ruelland, A. Dezetter, C. Puech and S. Ardoin Bardin, "Long term monitoring of land cover changes based on Landsat

- imagery to improve hydrological modelling in West Africa," *Int. J. Remote Sens.*, vol. 29, pp. 3533-3551, 2008.
- [26] P. Chen, X. Lu, S. Liew and L. Kwok, "Quantification of land cover change and its impact on hydro-geomorphic processes in the upper yangtze using multi-temporal landsat imagery: An example of the minjiang area," in *Geoscience and Remote Sensing Symposium, 2002. IGARSS'02. 2002 IEEE International*, 2002, pp. 1216-1218.
- [27] Geun-Won Yoon, Young Bo Yun and Jong-Hyun Park, "Change vector analysis: Detecting of areas associated with flood using landsat TM," in *Geoscience and Remote Sensing Symposium, 2003. IGARSS '03. Proceedings. 2003 IEEE International*, 2003, pp. 3386-3388 vol.5.
- [28] Wen Wang, Hai-Xu Hu and Juan Hu, "Land cover change detection based on MODIS 250m vegetation index time series data," in *Geoinformatics, 2009 17th International Conference on*, 2009, pp. 1-6.
- [29] Xi Wu-jun, Wang Jin-liang, Yang Bing-feng and Yang Wang-zhou, "ETM+ image classification research based on stratified and regional classification method--take land-use and land-cover in shangri-la for example," in *Information Engineering and Computer Science, 2009. ICIECS 2009. International Conference on*, 2009, pp. 1-4.
- [30] J. Malpica and M. Alonso, "A method for change detection with multi-temporal satellite images using the RX algorithm," *International Archives of Photogrammetry, Remote Sensing and Spatial Information Science, Beijing, China*, vol. 37, pp. 1631-1635.
- [31] V. Walter, "Object-based classification of remote sensing data for change detection," *ISPRS Journal of Photogrammetry and Remote Sensing*, vol. 58, pp. 225-238, 2004.
- [32] Yan Wang and M. Jamshidi, "Fuzzy logic applied in remote sensing image classification," in *Systems, Man and Cybernetics, 2004 IEEE International Conference on*, 2004, pp. 6378-6382 vol.7.
- [33] B. Al Momani, P. Morrow and S. McClean, "Knowledge-based semi-supervised satellite image classification," in *Signal Processing and its Applications, 2007. ISSPA 2007. 9th International Symposium on*, 2007, pp. 1-4.
- [34] K. J. Mackin, T. Yamaguchi, E. Nunohiro, Jong Geol Park, K. Hara, K. Matsushita, M. Ohshiro and K. Yamasaki, "Ensemble of artificial neural network based land cover classifiers using satellite data," in *Systems, Man and Cybernetics, 2007. ISIC. IEEE International Conference on*, 2007, pp. 1653-1657.
- [35] Yu Fu, Yuchun Wei, Chunmei Cheng, Yu Zhou and Lei Wang, "Extraction of land cover information based on decision tree method: A case of wuxi and changzhou city, china," in *Remote Sensing, Environment and Transportation Engineering (RSETE), 2011 International Conference on*, 2011, pp. 4054-4057.
- [36] Hybrid add
- [37] G. R. Gibson, "Three Decades of Agricultural Land Use and Land Cover Change in Iraq," *War and Agriculture: Three Decades of Agricultural Land use and Land Cover Change in Iraq*, 2012.
- [38] U.S Department of State, "Background Note: Iraq," vol. 2012, 2012.
- [39] BBC, "1988: Thousands die in Halabja gas attack "BBC News, -03-16, 1988.
- [40] A. A. Dlawer, "Death Clouds: Saddam Hussein's Chemical War Against the Kurds 5/1/1991 | Dlawer dot Net " vol. 2012, .
- [41] D. Hirst, "The Kurdish victims caught unaware by cyanide" *The Guardian*, , 1988, 1988.
- [42] H. Osman, "Iraqi Kurds recall chemical attack" *BBC News*, , 2002, 2002.
- [43] Susan F. Kinsley, "Whatever Happened To The Iraqi Kurds? (Human Rights Watch Report, March 11, 1991) " vol. 2012, 1991.
- [44] P. John, "Chemical Weapons Programs - Iraq Special Weapons Facilities " vol. 2012, .
- [45] R. S. Lunetta, D. M. Johnson, J. G. Lyon and J. Crotwell, "Impacts of imagery temporal frequency on land-cover change detection monitoring," *Remote Sens. Environ.*, vol. 89, pp. 444-454, 2004.
- [46] H. Wang and E. C. Ellis, "Image misregistration error in change measurements," *Photogramm. Eng. Remote Sensing*, vol. 71, pp. 1037, 2005.
- [47] D. Vanderzee and D. Ehrlich, "Sensitivity of ISODATA to changes in sampling procedures and processing parameters when applied to AVHRR time-series NDVI data," *Remote Sensing*, vol. 16, pp. 673-686, 1995.
- [48] J. T. Tou and R. C. Gonzalez, "Pattern recognition principles," *Image Rochester NY*, vol. 7, 1974.
- [49] J. A. Richards and X. Jia, *Remote Sensing Digital Image Analysis*. Springer Berlin et al., 1986.
- [50] T. M. Lillesand and R. W. Keifer, *Remote Sensing and Image Interpretation*, 1994.
- [51] C. Song, C. E. Woodcock, K. C. Seto, M. P. Lenney and S. A. Macomber, "Classification and Change Detection Using Landsat TM Data:: When and How to Correct Atmospheric Effects?" *Remote Sens. Environ.*, vol. 75, pp. 230-244, 2001.
- [52] G. Chander, B. L. Markham and D. L. Helder, "Summary of current radiometric calibration coefficients for Landsat MSS, TM, ETM , and EO-1 ALI sensors," *Remote Sens. Environ.*, vol. 113, pp. 893-903, 2009.
- [53] R. Irish, "Landsat 7 science data users handbook," *Landsat Project Science Office*, vol. 2008, 2008.
- [54] F. F. Sabin Jr, *Remote Sensing: Principles and Interpretation*, 1986.
- [55] J P. Aplin and P. M. Atkinson, "Predicting missing field boundaries to increase per-field classification accuracy," *Photogramm. Eng. Remote Sensing*, vol. 70, pp. 141-149, 2004.
- [56] A. Shalaby and R. Tateishi, "Remote sensing and GIS for mapping and monitoring land cover and land-use changes in the Northwestern coastal zone of Egypt," *Appl. Geogr.*, vol. 27, pp. 28-41, 2007.
- [57] G. M. Foody, "Status of land cover classification accuracy assessment," *Remote Sens. Environ.*, vol. 80, pp. 185-201, 2002.